PHYSICAL REVIEW B **90**, 140403(R) (2014)

# Theory of Mn-doped II-II-V semiconductors

J. K. Glasbrenner,[1] I. Žutić,[2] and I. I. Mazin[3]
[1]*National Research Council/Code 6393, Naval Research Laboratory, Washington, DC 20375, USA*
[2]*Department of Physics, University at Buffalo, State University of New York, New York 14260, USA*
[3]*Code 6393, Naval Research Laboratory, Washington, DC 20375, USA*

(Received 12 May 2014; revised manuscript received 15 September 2014; published 13 October 2014)

A recently discovered magnetic semiconductor $\mathrm{Ba_{1-x}K_x(Zn_{1-y}Mn_y)_2As_2}$, with its decoupled spin and charge doping, provides a unique opportunity to elucidate the microscopic origin of the magnetic interaction and ordering in dilute magnetic semiconductors (DMSs). We show that (i) the conventional density functional theory accurately describes this material, and (ii) the magnetic interaction emerges from the competition of the short-range superexchange and a longer-range interaction mediated by the itinerant As holes, coupled to Mn via the Schrieffer-Wolff $p$-$d$ interaction representing an effective Hund's rule coupling $J_H^{\mathrm{eff}}$. The key difference between the classical double exchange and the actual interaction in DMSs is that an effective $J_H^{\mathrm{eff}}$, as opposed to the standard Hund's coupling $J_H$, depends on the Mn $d$-band position with respect to the Fermi level, and thus allows tuning of the magnetic interactions. The physically transparent description of this material may also be applicable in more complicated DMS systems.

DOI: 10.1103/PhysRevB.90.140403 PACS number(s): 75.50.Pp, 75.30.Et, 75.50.Dd, 81.05.Hd

*Introduction*. The carrier-mediated magnetism in dilute magnetic semiconductors (DMSs) [1–5] offers a versatile control of the exchange interaction by tuning the Curie temperature $T_C$ through changes in the carrier density, for example by an applied electric field, photoexcitations, or even heating [5–8]. However, despite four decades of intensive work, challenges remain and materials complexity often hinders theoretical understanding. The origin of magnetic ordering [1–3,5] and paths to higher $T_C$ remain strongly debated [3,9,10].

Doping with Mn is the usual method for synthesizing DMS. In the II-VI DMSs $\mathrm{Mn^{2+}}$ is isovalent with the group II ions and provides only spin doping; the lack of carriers makes robust ferromagnetism elusive. In the most common III-V DMSs (the best studied example is GaAs:Mn) this leads to both spin and carrier doping, but a low solubility limit for Mn complicates growth and can lead to nanoscale clustering of Mn ions. This dual role of Mn complicates theoretical understanding, including whether double exchange [11] is a relevant mechanism in these systems. The argument against double exchange is that it requires either different charge states [12] on Mn and/or the presence of an impurity band [4], which is a misconception that we will address later in this Rapid Communication. The coupled spin and charge doping also creates difficulties in establishing the connection between host properties and figures of merit [13]. For example, a prediction of $T_C > 300$ K in GaN:Mn [14] has stimulated many efforts that turned out to be fruitless [15,16]. Finally, both substitutional and interstitial Mn are thermodynamically stable and form during synthesis, which additionally complicates theoretical treatment.

The recent discovery of the I-II-V and related II-II-V DMS compounds [17–19] provides a way to overcome these difficulties. In contrast to the II-VI and III-V compounds, in the II-II-V ones hole and spin doping are controlled separately by substitution with the group II and transition metal ions, respectively. In $\mathrm{(Ba_{0.7}K_{0.3})(Zn_{0.85}Mn_{0.15})_2As_2}$, a $T_C \sim 220$ K [20] is already higher than $\sim 190$ K [3] attained in GaAs:Mn. Unlike GaAs, both $p$- and $n$-doped II-II-V's can be ferromagnetic [19,21], and a coercive field $\sim 10^4$ Oe in $\mathrm{(Ba,K)(Zn,Mn)_2As_2}$ at 2 K [19] is two orders of magnitude larger than in GaAs:Mn. Apart from potential applications [5], the II-II-V DMSs are well suited for theoretical study because (1) the $\mathrm{Mn^{2+}}$ is isovalent with Zn, (2) charge is doped into the Ba sublayer, spatially and electronically disconnected from the active $\mathrm{(Zn,Mn)_2As_2}$ layers, and (3) interstitial locations for Mn ions are energetically precluded.

A key feature that a theory of II-II-V DMS must capture is the curious result that while the high-$T$ susceptibility indicates a high spin state with $5\mu_B$/Mn, the low-$T$ ferromagnetic magnetization corresponds to moments of $\lesssim 2\ \mu_B$ that depend on both Mn and K concentration. Reference [19] conjectured that this may be due to the formation of nearest-neighbor $\mathrm{Mn_2}$ singlets. We will show below that a simple, random statistical distribution of singlets, as initially suggested, cannot explain the Mn and K concentration dependency of the magnetization, while a distribution in thermodynamic equilibrium at temperatures consistent with experimental synthesis can. This finding paves the way towards synthesizing II-II-V DMS materials with larger magnetizations, important, for example, in spintronics [5].

In this Rapid Communication, we present density functional theory (DFT) calculations of the energetics of various Mn pairs in the Zn sublattice. We then extract exchange parameters and find that ordering changes from antiferomagnetic (AFM) with no hole doping to ferromagnetic (FM) with hole doping, with the exception of nearest-neighbor (NN) pairs, which remain AFM and are energetically preferred. We then show using thermodynamic arguments that singlet formation is responsible for the reduced magnetization in Ref. [19]. We also address the different terminologies used for the effective magnetic interaction between the Mn $d$ and As $p$ states, such as double exchange [11], the Zener $p$-$d$ model [22], and the Ruderman-Kittel-Kasuya-Yosida (RKKY) interaction [23–25]. This controversy over the exchange mechanism can be resolved here because this recently discovered class of

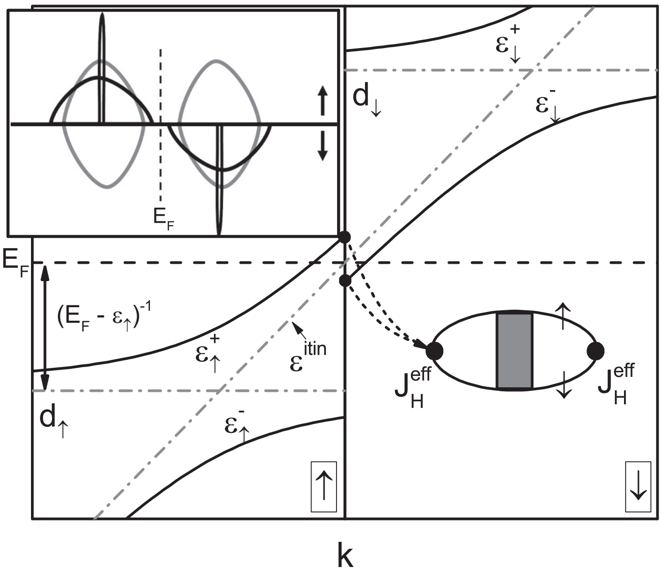

FIG. 1. A cartoon of the interaction between localized spins mediated by the itinerant carriers depicting a spin-resolved schematic of the broad As band $\varepsilon^{\text{itin}}$ hybridizing with the narrow Mn bands $d_\uparrow$ and $d_\downarrow$, forming the bands $\varepsilon^{\pm}_{\uparrow,\downarrow}$. The effective magnetic coupling $J_H^{\text{eff}}$ scales with $(E_F - \varepsilon_\uparrow)^{-1}$. Inset: A schematic of the $\text{BaZn}_2\text{As}_2$ DOS before (gray lines) and after (black lines) Mn doping. The narrow Mn states interact with the As states, broadening the DOS and reducing the indirect band gap.

DMS systems allows one to treat spin and charge doping independently and the system does not have an impurity band at the Fermi level nor mixed charge states for Mn. In our view, contrary to the argument that double exchange is irrelevant and the Zener *p*-*d* model is fundamentally different, the situation is instead that these all describe the same indirect exchange interaction [26] and therefore the same basic physics.

*Calculations*. We employed two DFT implementations: a pseudopotential method (VASP [27,28]) and an all-electron method (ELK) [29]. Selected results have been verified against an alternative package, WIEN2K [30]. A generalized gradient approximation [31] was used for total energy calculations and the modified Becke-Johnson functional [32,33] (known to give correct band gaps for semiconductors) was used for analyzing the electronic structure. For pure $\text{BaZn}_2\text{As}_2$ we obtain an indirect gap of 0.25 eV between the Γ and $Z$ points, and a direct gap of 0.71 eV at the Γ point, in agreement with previous calculations [34] (see the Supplemental Material [35]).

We first analyze the effect of Mn doping $[\text{Ba}(\text{Zn}_{1-\text{y}}\text{Mn}_\text{y})_2\text{As}_2, y > 0]$. The inset in Fig. 1 qualitatively illustrates the spin-resolved density of states (DOS) (see the Supplemental Material [35] for explicit DOS calculations). There are five Mn bands in each spin, confirming the $\text{Mn}^{2+}$ state. The calculated Mn moment is $\sim 4.7\mu_B$ in ELK and $\sim 4.9\mu_B$ in VASP [36]. The valence band is predominantly As $p$ states, and the conductance band Ba states. The As states hybridize with Mn (Fig. 1), as parametrized by hopping $t_{pd}$ [37]. As a result, the top of the As spin-majority band (↑ band) is pushed up and the bottom down at a rate of $\sim 2.8y$ eV, so for $y = 0.25$, there is a shift of 0.7 eV. In contrast, the bottom of the conductance (Ba) spin-minority band (↓ band) is pushed down because of the hybridization with unoccupied Mn states. This provides the magnetic coupling between the local spin and itinerant carriers [38]. Another manifestation of the same effect, verifiable experimentally, is that with Mn doping the indirect gap between the top of the valence ↑ band and the bottom of the conduction ↓ band is reduced and eventually closes when the doping is large enough (see the inset of Fig. 1).

Upon hole doping $[\text{Ba}_{1-\text{x}}\text{K}_\text{x}(\text{Zn}_{1-\text{y}}\text{Mn}_\text{y})_2\text{As}_2, x > 0]$, the calculated Mn moments are reduced (by 40% at $x = 0.4$) and As atoms acquire opposite moments (Ba and Zn remain unpolarized). Both effects are caused by the Mn-As hybridization, while K doping makes the effect visible. Indeed, because of the upshift of the top of the As band, there are more holes in its ↑ states, creating negative polarization on As. Furthermore, because of proximity to the Mn ↑ states, the hybridization of As holes with them is stronger than with the ↓ states, so holes carry more Mn ↑-band character and hole doping reduces the Mn moments.

Next we constructed different supercells, placing Mn pairs into different substitutional positions. Unlike GaAs:Mn, where Mn easily occupies interstitials, complicating the theoretical analysis, in $\text{BaZn}_2\text{As}_2$ this is essentially impossible. The calculated free-energy penalty for interstitial versus substitutional Mn doping is huge, $F_{\text{int}} - F_{\text{sub}} > 2.4$ eV/Mn, for all admissible values of the Zn chemical potential (see the Supplemental Material [35]).

We now assume a Heisenberg model for the Mn-Mn interactions at the sites $i, j$,

$$H = \sum_{i<j} J_x^{ij} \hat{S}_i \cdot \hat{S}_j, \tag{1}$$

where the $\hat{S}_{i,j}$ are the unit vectors in the spin directions. We can map the calculated energies for different magnetic configurations onto Eq. (1) and extract the spatial dependence of the exchange $J_x^{ij}$.

Figure 2(a) summarizes $J_x^{ij}$ for both intraplanar and interplanar Mn pairs up to seven neighbors for $x = 0$, 0.2, and 0.4 hole dopings (for more details, see the Supplemental Material [35]). We note that the intraplanar and interplanar results roughly lie on the same universal curve, so we define $J_x(r) \equiv J_x^{ij}$. Without hole doping ($x = 0$), $J_x(r)$ is AFM for all pairs and decays strongly with distance, consistent with superexchange [11,26].

Hole doping drives the system toward ferromagnetism, so that $J_x(r)$ becomes FM for second and higher neighbors. For NN pairs, $J_x(r)$ remains AFM even for $x = 0.4$, but is reduced threefold. This reduction, along with the second neighbor's exchange parameter barely changing sign to become FM for $x = 0.2$, reveals that this behavior is due to the competition between the short-range AFM superexchange and a longer-range FM interaction.

We now address the puzzling reduction of the net magnetization $M$ compared with the local Mn moments. We verified that even for $x = 0.4$ doping that the NN exchange parameter is AFM, such that NN Mn pairs form a singlet. Let us first assume that Mn dopants are randomly distributed in the Zn lattice and estimate the magnetization reduction. If we neglect clusters of three or more Mn atoms (i.e., assuming

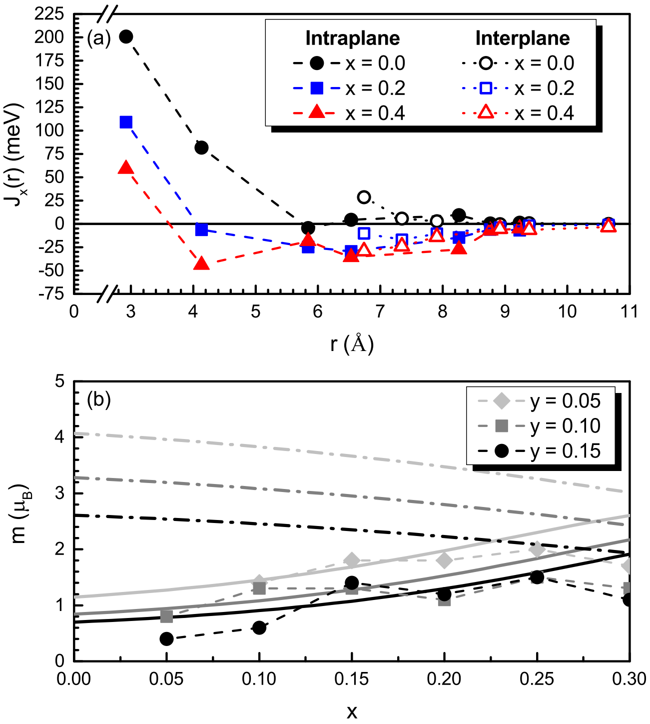

FIG. 2. (Color online) (a) The exchange coupling $J_x(r)$ as a function of distance between Mn pairs for different hole dopings $x$. (b) The dependence of the reduced magnetization due to singlet formation on hole doping. The experimental points are from Ref. [19]. The solid lines are the reduced magnetization when Mn singlet formation is in thermodynamic equilibrium at 500 K, while the dashed-dotted lines are the reduced magnetization for a random distribution of Mn atoms. The light gray, dark gray, and black lines correspond to $y = 0.05$, 0.10, and 0.15, respectively.

$y \ll 1$), we obtain $M_{\text{theor}}(x,y) = M(x)(1-y)^4$. Depending on $x$, $M(x) \approx 3$–$5\mu_B$, and we can interpolate $M(x)$ using our results. Figure 2(b) shows $M_{\text{theor}}(x,y)$ for three values of $y$ (dashed-dotted lines) and compares it with the experiment of Ref. [19]. While there is some qualitative agreement, the magnetization suppression is noticeably underestimated, especially for small $x$.

Our calculations also indicate an energetic preference for NN Mn pairs to form. This, along with the variation in experimental Mn moments, leads us to conclude that the suppression is sensitive to sample preparation and hence the Mn distribution is not entirely random. To quantify this, we use the calculated energy differences between the AFM NN pair and a remote FM pair: $\Delta E(x) \sim 185$, 80, and $-30$ meV, for $x = 0$, 0.2, and 0.4, respectively. We can now evaluate the free energy using these values and the combinatorial entropy (see the Supplemental Material [35]) to obtain the moment reduction $r = (\sqrt{\beta^2 + 16\beta y} - \beta)/8y$, correct in the $y \ll 1$ limit, where $\beta = \exp[-\Delta E/T]$. Interpolating the calculated $\Delta E(x)$ and $M(x)$, and using as the effective synthesis temperature 500 K [39], we get the solid lines shown in Fig. 2(b). Given the variation in the experimental data and the lack of any adjustable parameter, the agreement is excellent. It is worth noting that it is not well accepted that DFT can be used to make useful predictions for DMS systems [4,12,40], so this success demonstrates that DFT analysis has a strong role to play in understanding this recently discovered class of systems. From these calculations we can predict that quenching, rather than slow cooling, may be advantageous for enhancing the magnetization per Mn, which can be as high as $3\mu_B$.

*Discussion.* We determined that the magnetic ordering is a combination of a short-range AFM interaction and a longer-range FM interaction. We identify the AFM interaction as superexchange, which is compatible with Mn being in the high-spin $S = 5/2$ state, and is accounted for in DFT. The basic picture of superexchange is that there is an effective amplitude $\tilde{t}_{dd}$ for a $d$ electron to hop from one Mn to another. For NN pairs $t$ is large, as only one intermediate hop to an As $p$ state is required, and in addition there is some direct overlap between Mn $d_{x^2-y^2}$ orbitals. If the alignment is FM, hopping leads to a splitting of the occupied Mn states with no gain in kinetic energy. For an AFM alignment, where hopping proceeds from occupied to unoccupied states, this leads to a downshift of the occupied Mn states by $2\tilde{t}_{dd}^2/U$, where $U$ is the energy cost of flipping the spin of one $d$ electron. This cost in DFT is $\sim 5J_H$, where $J_H \sim 0.8$ eV is the Hund's rule coupling in Mn (in the Hubbard model $U$ comes from the Coulomb repulsion and may be larger than $5J_H$). This creates the superexchange coupling $J_{\text{SE}} \approx 2\tilde{t}_{dd}^2/U$. For farther neighbors the hopping probability involves multiple hoppings via high-lying Zn states and rapidly decays.

We will argue now [41] that the long-range FM ordering is a version of double exchange (DE) [11], but first we give an overview of the DE interaction. The original model [22] assumed a strong Hund's coupling between localized spins and itinerant electrons from the same atomic species, which in practice is due to noninteger valency, and has led to the misconception that DE itself *requires* mixed valency. Instead, the only real requirement is that the interaction of the local spins with itinerant electrons be described by an operator of the form $J_H \hat{S} \cdot \hat{\sigma}$. Note that the nature and sign of $J_H$ does not matter, because in the end $J_H$ is squared.

The other essential ingredient of DE was the itinerant carriers delocalizing to lower their kinetic energy, which preferred a FM arrangement of the local spins. In the original model [22] the strong coupling limit $J_H \to \infty$ was assumed in order to simplify the calculations, but that was not a necessary condition for DE. The DE picture, that of itinerant electrons adjusting their spin density to the background of local spins with some configurations being more energetically preferable, is simply the standard spin response theory described in the weak coupling regime by the linear spin susceptibility $\chi(q)$. In general, $\chi(q)$ depends on the electronic structure and Fermi surface geometry, so again for simplicity it is often approximated by its value at the $\Gamma$ point, $\chi(q) = \chi(0) = N_\uparrow(0)$, which is not a bad approximation when all sites contain a local moment. Again, we note that this approximation is not essential when defining DE. Finally, if the concentration of itinerant carriers is small such that $2\pi/k_F \gg d$ ($d$ is the average distance between spins), then the response is FM for all relevant distances. For larger $d$ the response decays rapidly and might acquire an oscillatory part, which depends on the Fermi surface. This is known as the RKKY interaction [23–25].

To review, the general picture is that the DE implies a local spin interacting with an itinerant sea of carriers, which itself responds by adjusting its spin density to align with the other localized spins, and then another of these localized spins interacts locally with the sea. There are two local exchange processes involved (see the diagram in Fig. 1), hence DE. In other words, DE and RKKY are two different sides of the same coin.

With this clarified, we now turn to the details of the effective exchange interaction between the local Mn spins and itinerant As holes. As discussed, in DFT the As electrons at the Fermi level hybridize with Mn and acquire spin splitting (see Fig. 1). The upshift of ↑ states at the Fermi energy is $5Zt_{pd}^2/(E_F - \varepsilon_\uparrow)$ (the bottom of the As band shifts *down*), where $Z = 4$ is the Mn-As coordination number. Here the Mn ↓ states are located at $\varepsilon_\downarrow > E_F$, and the ↑ states at $\varepsilon_\uparrow < E_F$, and, for simplicity, the hopping $t_{pd}$ is assumed to be the same for all Mn $d$ states. Similarly, the ↓ bands are shifted down by $5Zt_{pd}^2/(\varepsilon_\downarrow - E_F)$. This yields an effective Mn spin splitting and thus an effective Hund's rule coupling of

$$J_H^{\rm eff} = \frac{-Zt_{pd}^2(\varepsilon_\uparrow - \varepsilon_\downarrow)}{(E_F - \varepsilon_\uparrow)(\varepsilon_\downarrow - E_F)} = \frac{-Zt_{pd}^2 U}{(E_F - \varepsilon_\uparrow)(\varepsilon_\uparrow + U - E_F)}.$$

This is formally the same as the Schrieffer-Wolff transformation frequently used for Kondo systems [11,38]. The DMS literature typically refers to this as the $p$-$d$ model. We emphasize that the $p$-$d$ model [26] is not an alternative to DE, but a modification of the latter, where $J_H$ is replaced with $J_H^{\rm eff}$. The RKKY theory is in the same spirit, modifying the same physics in a different way by lifting the $q = 0$ approximation, in weak coupling, and using a $q$-dependent susceptibility. In all cases the effective coupling appears as a pair of vertices attached to a polarization bubble as in Fig. 1, and so the sign of $J_H^{\rm eff}$ is irrelevant.

Unlike $J_{H,}$ $J_H^{\rm eff}$ is, in principle, tunable by changing the $U$ and the position of the occupied $d$-level $\varepsilon_\uparrow$. In our DFT calculations $E_F - \varepsilon_\uparrow \sim U/2$, the least advantageous regime. We suggest that substituting As with Sb or P may shift $\varepsilon_\uparrow$ up or down, yielding a $E_F - \varepsilon_\uparrow$ closer to $U/5$ or $4U/5$ and increasing $J_H^{\rm eff}$ by $\sim 60\%$. Assuming that other parameters remain unchanged, an enhancement of exchange coupling could increase $T_C$ by a factor of 2.5, suggesting a path to room-temperature FM ordering.

*Conclusions.* We have shown, based on our first principles calculations, that ferromagnetism in (Ba,K)(Zn,Mn)$_2$As$_2$ is a result of the interaction of localized Mn spins with itinerant As holes that have a ferromagnetic spin response for all relevant Mn-Mn distances, except for nearest neighbors. This is a variant of the classical double exchange with the simple modification of replacing the Hund's coupling $J_H$ by the effective $p$-$d$ coupling $J_H^{\rm eff}$.

The nearest-neighbor magnetic interaction is a combination of superexchange that is weakened, but not overcome, by the ferromagnetic double exchange, and for a K concentration less than ∼0.35 it is energetically advantageous for Mn to form nearest-neighbor singlet pairs. Our calculations describe this process quantitatively and predict a net magnetization reduction from the ideal $5\mu_B$/Mn, in excellent agreement with experiment.

While our findings have focused on the (Ba,K)(Zn,Mn)$_2$As$_2$ compound, we believe that the transparent and simple physical picture that has emerged from studying this unique system is more general and applicable to other DMS compounds. Our theory and calculations are uncomplicated by multiple chemical issues common to other families of DMSs. Indeed, the excellent agreement with experiment confirms that DFT should be considered a valuable tool for understanding DMS systems. Thus, this recently discovered generation of DMSs is an exciting playground for experimentalists and theorists alike and deserves further study to elucidate the intrinsic physics of DMS materials.

*Acknowledgments.* We are grateful to A. Petukhov, F. Ning, and C. Q. Jin for their useful discussions. I.I.M. acknowledges funding from the Office of Naval Research (ONR) through the Naval Research Laboratory's Basic Research Program. J.K.G. acknowledges the support of the NRC program at NRL. I.Z. was supported by DOE-BES Grant No. DE-SC0004890 (theory) and ONR Grant No. N000141310754 (applications).

---

[1] J. K. Furdyna, J. Appl. Phys. **64**, R29 (1988).
[2] H. Ohno, Science **281**, 951 (1998).
[3] T. Dietl, Nat. Mater. **9**, 965 (2010).
[4] T. Jungwirth, J. Sinova, J. Mašek, J. Kucera, and A. H. MacDonald, Rev. Mod. Phys. **78**, 809 (2006).
[5] I. Žutić, J. Fabian, and S. D. Sarma, Rev. Mod. Phys. **76**, 323 (2004).
[6] S. Koshihara, A. Oiwa, M. Hirasawa, S. Katsumoto, Y. Iye, C. Urano, H. Takagi, and H. Munekata, Phys. Rev. Lett. **78**, 4617 (1997).
[7] H. Ohno, D. Chiba, F. Matsukura, T. O. E. Abe, T. Dietl, Y. Ohno, and K. Ohtani, Nature (London) **408**, 944 (2000).
[8] A. G. Petukhov, I. Žutić, and S. C. Erwin, Phys. Rev. Lett. **99**, 257202 (2007).
[9] M. Tanaka, S. Ohya, and P. N. Hai, Appl. Phys. Rev. **1**, 011102 (2014).
[10] M. Dobrowolska, K. Tivakornsasithorn, X. Liu, J. Furdyna, M. Berciu, K. M. Yu, and W. Walukiewicz, Nat. Mater. **11**, 444 (2012).
[11] D. Khomskii, *Basic Aspects of the Quantum Theory of Solids* (Cambridge University Press, Cambridge, U.K., 2010).
[12] T. Dietl and H. Ohno, Rev. Mod. Phys. **86**, 187 (2014).
[13] S. C. Erwin and I. Žutić, Nat. Mater. **3**, 410 (2004).
[14] T. Dietl, H. Ohno, F. Matsukura, J. Cibert, and D. Ferrand, Science **287**, 1019 (2000).
[15] K. Sato, L. Bergqvist, J. Kudrnovský, P. H. Dederichs, O. Eriksson, I. Turek, B. Sanyal, G. Bouzerar, H. Katayama-Yoshida, V. A. Dinh, T. Fukushima, H. Kizaki, and R. Zeller, Rev. Mod. Phys. **82**, 1633 (2010).
[16] M. Sawicki, T. Devillers, S. Galeski, C. Simserides, S. Dobkowska, B. Faina, A. Grois, A. Navarro-Quezada, K. N. Trohidou, J. A. Majewski, T. Dietl, and A. Bonanni, Phys. Rev. B **85**, 205204 (2012).

[17] Z. Deng, C. Q. Jin, Q. Q. Liu, X. C. Wang, J. L. Zhu, S. M. Feng, L. C. Chen, R. C. Yu, C. Arguello, T. Goko, F. Ning, J. Zhang, Y. Wang, A. A. Aczel, T. Munsie, T. J. Williams, G. M. Luke, T. Kakeshita, S. Uchida, W. Higemoto, T. U. Ito, B. Gu, S. Maekawa, G. D. Morris, and Y. J. Uemura, Nat. Commun. **2**, 422 (2011).

[18] Z. Deng, K. Zhao, B. Gu, W. Han, J. L. Zhu, X. C. Wang, X. Li, Q. Q. Liu, R. C. Yu, T. Goko, B. Frandsen, L. Liu, J. Zhang, Y. Wang, F. L. Ning, S. Maekawa, Y. J. Uemura, and C. Q. Jin, Phys. Rev. B **88**, 081203 (2013).

[19] K. Zhao, Z. Deng, X. C. Wang, W. Han, J. L. Zhu, X. Li, Q. Q. Liu, R. C. Yu, T. Goko, B. Frandsen, L. Liu, F. Ning, Y. J. Uemura, H. Dabkowska, G. M. Luke, H. Luetkens, E. Morenzoni, S. R. Dunsiger, A. Senyshyn, P. Böni, and C. Q. Jin, Nat. Commun. **4**, 1442 (2013).

[20] K. Zhao, B. Chen, G. Q. Zhao, X. Li, Z. Yuan, Z. Deng, Q. Q. Liu, and C. Q. Jin, Chin. Sci. Bull. **59**, 2524 (2014).

[21] H. Man, C. Ding, S. Guo, G. Zhi, X. Gong, Q. Wang, H. Wang, B. Chen, and F. L. Ning, arXiv:1403.4019.

[22] C. Zener, Phys. Rev. **82**, 403 (1951).

[23] M. A. Ruderman and C. Kittel, Phys. Rev. **96**, 99 (1954).

[24] T. Kasuya, Prog. Theor. Phys. **16**, 45 (1956).

[25] K. Yosida, Phys. Rev. **106**, 893 (1957).

[26] E. L. Nagaev, *Physics of Magnetic Semiconductors* (Mir, Moscow, 1983).

[27] G. Kresse and J. Hafner, Phys. Rev. B **47**, 558(R) (1993).

[28] G. Kresse and J. Furthmüller, Phys. Rev. B **54**, 11169 (1996).

[29] ELK FP-LAPW code, http://elk.sourceforge.net/.

[30] P. Blaha, K. Schwarz, G. K. H. Madsen, K. Kvasnicka, and J. Luitz, *Computer code WIEN2K* (Karlheinz Schwarz, Techn. Universität Wien, Austria, 2001).

[31] J. P. Perdew, K. Burke, and M. Ernzerhof, Phys. Rev. Lett. **77**, 3865 (1996).

[32] A. D. Becke and E. R. Johnson, J. Chem. Phys. **124**, 221101 (2006).

[33] F. Tran and P. Blaha, Phys. Rev. Lett. **102**, 226401 (2009).

[34] I. R. Shein and A. L. Ivanovskii, J. Alloys Compd. **583**, 100 (2014).

[35] See Supplemental Material at http://link.aps.org/supplemental/10.1103/PhysRevB.90.140403 for additional details about the DFT calculations and the electronic structure, the fitting procedure to the Heisenberg Hamiltonian, an explicit derivation of the Mn-Mn pair distribution, and an analysis showing that interstitial Mn impurities are unstable.

[36] The difference is due to different space partitioning in different codes.

[37] While hopping in reality differs from orbital to orbital, for our purpose one effective parameter is sufficient.

[38] J. Cibert and D. Scalbert, in *Spin Physics in Semiconductors*, edited by M. I. Dyakonov, Springer Series in Solid-State Sciences Vol. 157 (Springer, Berlin, 2008), Chap. 13, pp. 389–431.

[39] The actual protocol involves a long annealing at $T \approx 1000$ K and then a very slow cooling to 300 K [19].

[40] J. Fujii, B. R. Salles, M. Sperl, S. Ueda, M. Kobata, K. Kobayashi, Y. Yamashita, P. Torelli, M. Utz, C. S. Fadley, A. X. Gray, J. Braun, H. Ebert, I. Di Marco, O. Eriksson, P. Thunström, G. H. Fecher, H. Stryhanyuk, E. Ikenaga, J. Minár, C. H. Back, G. van der Laan, and G. Panaccione, Phys. Rev. Lett. **111**, 097201 (2013).

[41] Similar reasoning has been put forth before [see H. Akai, Phys. Rev. Lett. **81**, 3002 (1998)].